Supporting Information

Hierarchical NiCo$_2$O$_4$ nanosheets on carbon nanofiber films for high energy density and long-life Li-O$_2$ batteries

Guoxue Liu, Lei Zhang*, Suqing Wang, Liang-Xin Ding, Haihui Wang*

G. Liu, Prof. L. Zhang, Dr. S. Wang, Prof. L. X. Ding, Prof. H. Wang

School of Chemistry and Chemical Engineering, South China University of

Technology, Guangzhou 510640, China

E-mail: celeizhang@scut.edu.cn; hhwang@scut.edu.cn

1. Experimental section

1.1 The synthesis of carbon nanofiber films

The carbon nanofibers derived from polyacrylonitrile were fabricated by an electrospining technique followed by stabilization and carbonization. Typically, 1.0 g of polyacrylonitrile (PAN) was dissolved in 10 mL of N, N-dimethylformamide (DMF) to form a homogeneous solution. The electrospun nanofibers were prepared with a voltage of 15 kV and collected by a metal drum. Then, the polymer nanofibers were stabilized at 280 $^{\circ}$C for 3 h in air. After stabilization, the nanofibers were carbonized at 1000 $^{\circ}$C for 2 h in a nitrogen atmosphere.

1.2 The synthesis of NiCo$_2$O$_4$@CNFs

The porous NiCo$_2$O$_4$ nanosheets were grown on the electrospun carbon nanofibers substrate by a simple hydrothermal method. Briefly, 0.001 M of Ni(NO$_3$)$_2$ 6H$_2$O, 0.002 M Co(NO$_3$)$_2$ 6H$_2$O and 0.008 M hexamethylene-tetramine (HTMA) were dissolved in 60 mL of H$_2$O with 20 mL of ethanol. Subsequently, the carbon nanofiber substrate was dipped into the prepared homogeneous solution for 1 h. The solution with the carbon nanofiber substrate was transferred into a Teflon-lined stainless-steel autoclave, which was sealed and kept at 90 $^{\circ}$C for 24 h. Afterward, the substrate was washed with ethanol and distilled water, and dried at 60 $^{\circ}$C overnight under vacuum. Finally, the Ni-Co precursor nanosheets on the carbon nanofiber substrate were transformed into porous NiCo$_2$O$_4$ nanosheets via annealing in a nitrogen atmosphere at 350 $^{\circ}$C for 2 h at a heating rate of 5 $^{\circ}$C min^{-1}.

1.3 Materials Characterization

The morphology and crystal structure of all materials were characterized by field-emission scanning electron microscope (FESEM; NOVA NANOSEM 430), transmission electron microscope (TEM; JEOL JEM-2100F), and X-ray diffraction (XRD; Bruker D8 Advance). Thermogravimetric analysis (TGA) was measured on the STA449 instrument with a ramp rate of 10 °C min^{-1} under an air atmosphere. The surface area analysis was measured on the Micromeritics ASAP 2460 instrument.

1.4 Electrochemical Measurements

The electrochemical properties of Li-O_2 batteries were measured by a 2032-type coin cell assembled in a glove box with an Ar atmosphere. The NiCo$_2$O$_4$@CNFs cathodes were fabricated by cutting a disk at a diameter of 8 mm. The same procedure was applied to fabricate pure carbon nanofiber electrode. The Li-O_2 cells consist of a cathode electrode, a glass fiber membrane separator (Whatman/F), an anode (Li-metal foil), and an electrolyte solution (1 M LiTFSI/TEGDME). The galvanostatical discharge and charge tests of the Li-O_2 cells were measured on a Neware Battery Testing System at room atmosphere within a voltage window of 2.00 − 4.50 V (versus Li/Li$^+$). Cyclic voltammetry tests were performed at a rate of 0.1 mV s^{-1} within the potential range of 2.00 to 4.50 V (*versus* Li/Li$^+$) by an electrochemical workstation (IM 6ex).

2. Calculation of theoretical energy density of Li$_2$O$_2$

Theoretical gravimetric capacity of Li$_2$O$_2$ can be calculated by using Faraday's law:[S1]

$$\rho^*_{Li_2O_2} = \frac{F \times Z_r}{M} = 1168.5 \; Ah/kg_{Li_2O_2}$$

$$F = 96485 \; C/mol = 26.80 \; Ah/mol$$

$$Z_r = 2 electrons, \; unitless$$

$$M = 45.88 \times 10^{-3} \; kg_{Li_2O_2}/mol$$

Theoretical energy density of Li_2O_2 can be calculated by multiplying the theoretical gravimetric capacity by the theoretical discharge voltage for Li-O_2 batteries (3.0 V vs. Li):[S2]

$$E_{Theoretical} = \rho^*_{Li_2O_2} \times V_{Theoretical} = 1168.5 \; Ah/kg_{Li_2O_2} \times 3.0 V vs. Li = 3505 \; Wh/kg_{Li_2O_2}$$

3. Calculation of Gravimetric Capacity

Gravimetric capacities are calculated by normalizing the measured charge from galvanostatic testing, $q_{measured}$, by either the mass of oxygen electrode (carbon), m_{oe} (m_c), or the mass of the discharge electrode, $m_{oe}+m_{Li2O2}$.

$$q_c = \frac{q_{measured}}{m_c} \; [mAh/g_c]$$

$$q_{gravimetric} = q_{oe+Li_2O_2} = \frac{q_{measured}}{m_{oe} + q_{measured}/\rho^*_{Li_2O_2}} \; \left[mAh/g_{oe+Li_2O_2} \right]$$

$$\rho^*_{Li_2O_2} = 1168.5 \left[mAh/g_{Li_2O_2} \right]$$

$$q_{measured} \equiv [mAh]$$

$$m_c \equiv [g]$$

$$m_{oe} \equiv [g]$$

The average mass of the $NiCo_2O_4$@CNFs cathode in this work was found to be 0.167 mg (~0.334 mg cm^{-2}) and the carbon mass was 0.1 mg, whereas the average mass of Li_2O_2 discharge product, corresponding to the average low rate (100 mA g^{-1}) discharge capacity (4179mA h g$^{-1}_c$), was found to be 0.358 mg$_{Li2O2}$. And the gravimetric capacity,

$q_{gravimetric}$, was found to be 796.4 mA h g$^{-1}_{oe+Li2O2}$.

4. Calculation of Practical energy density of the NiCo$_2$O$_4$@CNFs cathode

Practical energy density of oxygen electrodes can be calculated by multiplying the gravimetric capacity by the operating discharge voltage for Li-O$_2$ batteries:

$$E_{Pr\ actical}\ =\ q_{Gravimetric}\ \times\ V_{operating}\ =\ 796.4 kg_{oe+Li_2O_2}\ \times\ 2.65 V vs. Li\ =\ 2110\ Wh/kg_{oe+Li_2O_2}$$
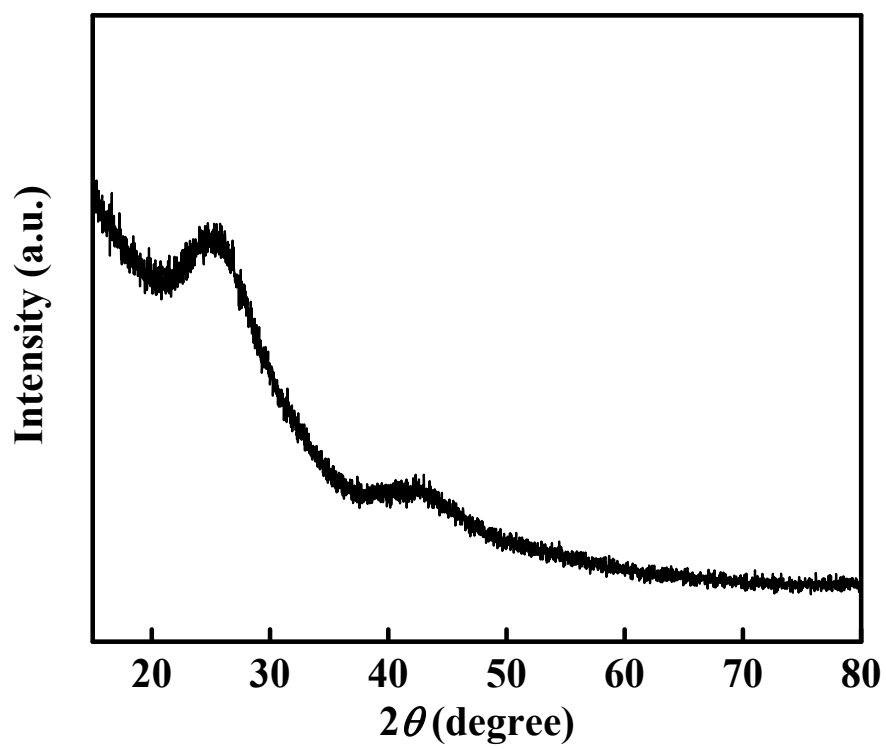
Fig. S1 XRD pattern of carbon nanofiber films (CNFs).
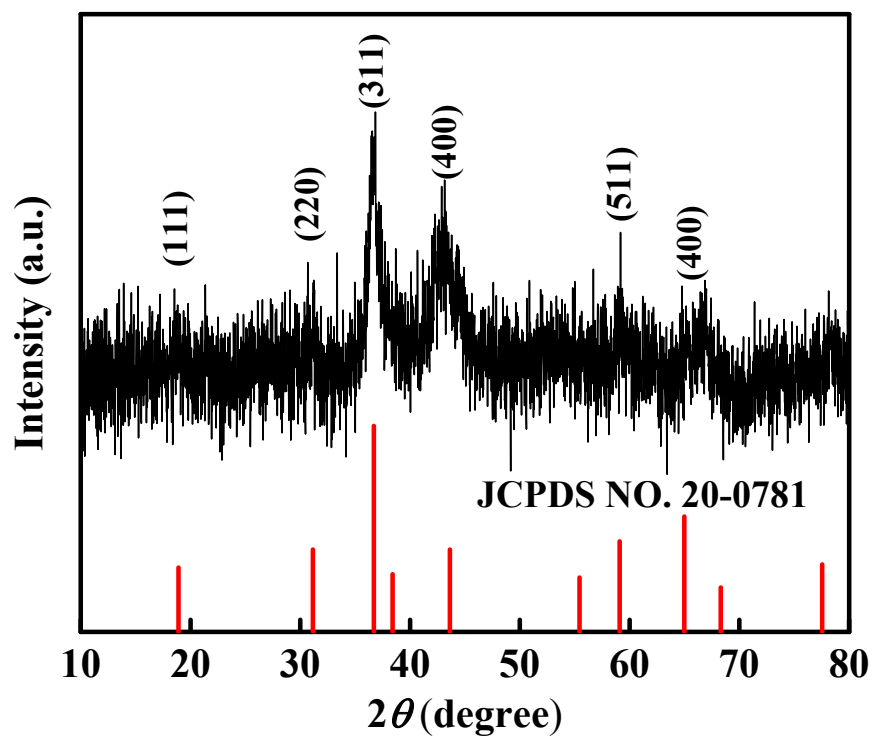
Fig. S2 XRD pattern of NiCo$_2$O$_4$ nanosheets scratched from carbon nanofiber films.
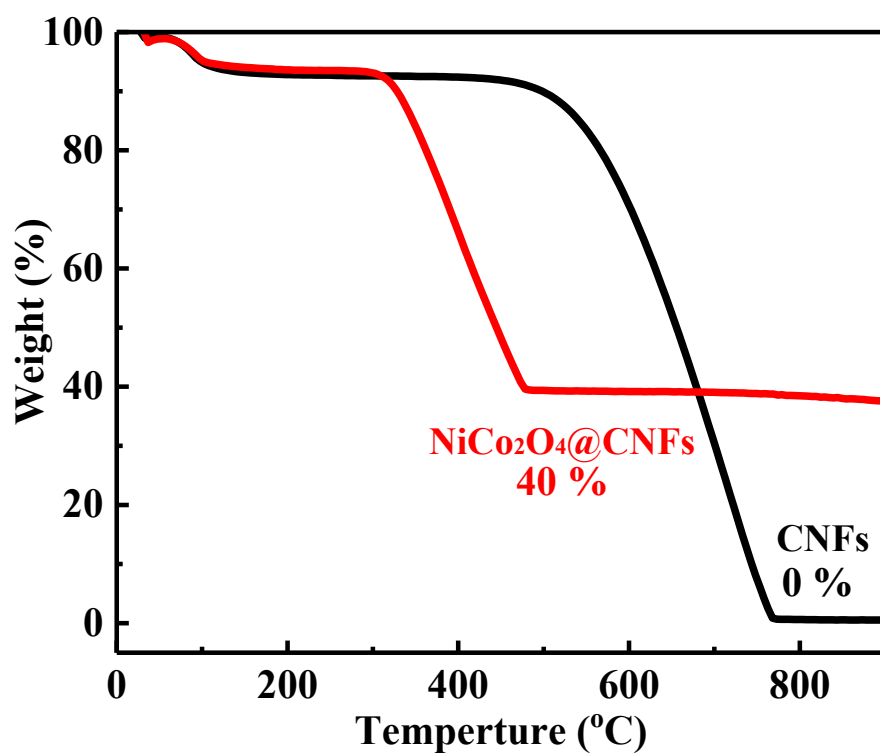
Fig. S3 TG curves of NiCo$_2$O$_4$@CNFs and CNFs.

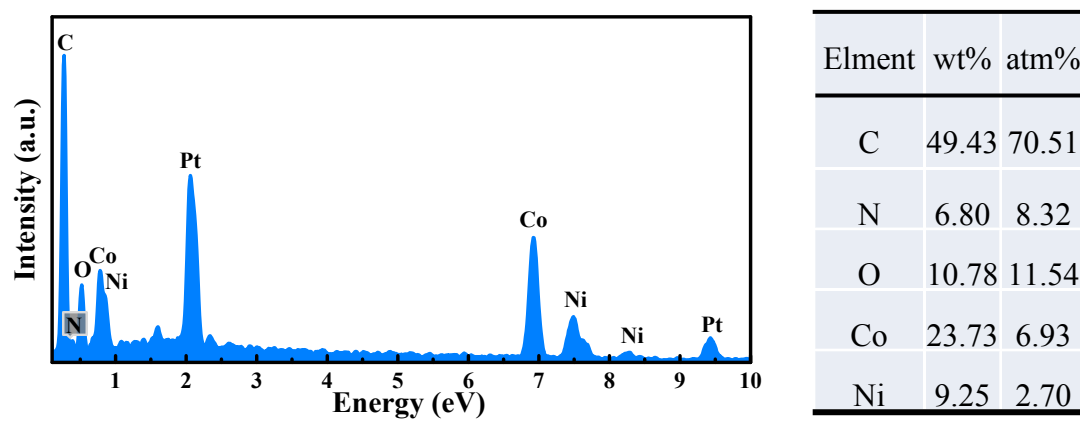| Elment	wt%	atm%
C	49.43	70.51
N	6.80	8.32
O	10.78	11.54
Co	23.73	6.93
Ni	9.25	2.70

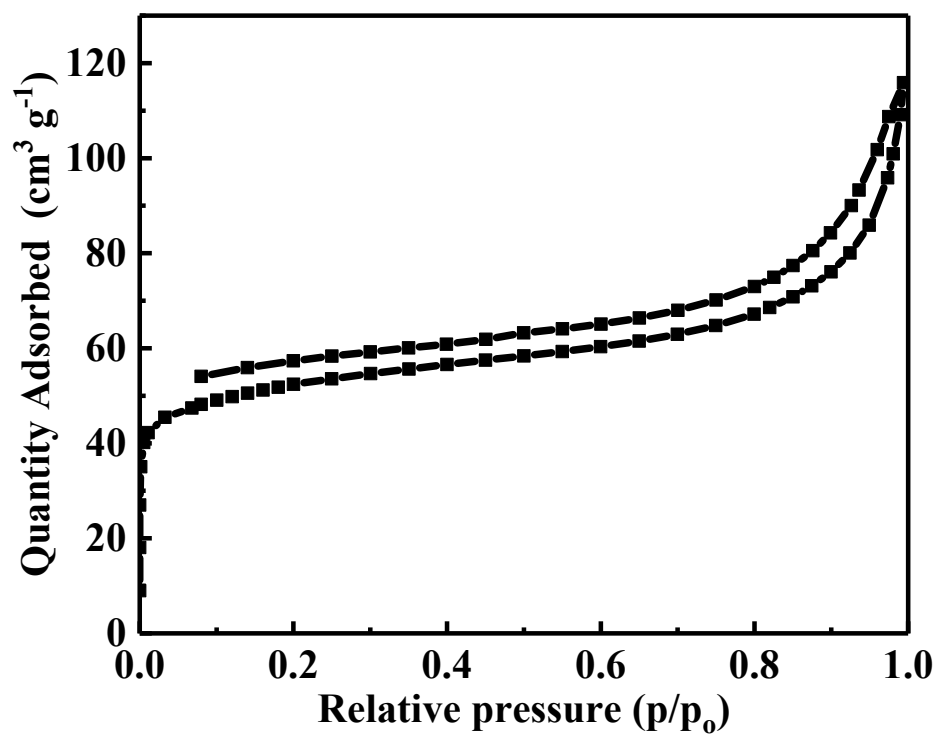**Fig. S4** EDX spectra of NiCo$_2$O$_4$@CNFs.

Fig. S5 Nitrogen adsorption desorption isotherms of $NiCo_2O_4$ nanosheets scratched

from carbon nanofiber films.

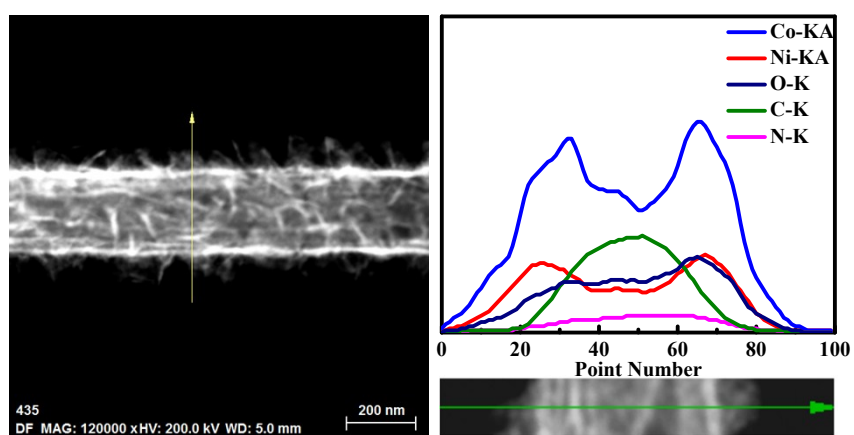**Fig. S6** STEM and corresponding Energy-dispersive X-ray (EDX) spectra line scans
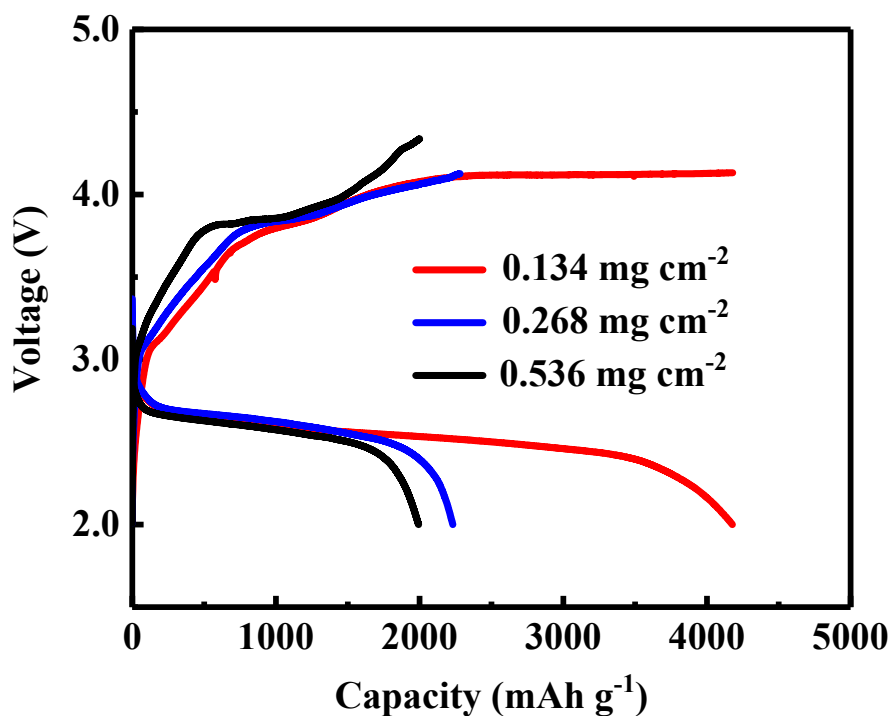
of NiCo$_2$O$_4$@CNFs.

Fig. S7 Initial discharge/charge curves of Li-O$_2$ batteries for the NiCo$_2$O$_4$@CNFs cathode with loading mass of 0.134, 0.268, 0.536 mg cm^{-2} at the same mass current density.

In order to further investigate the electrochemical performance of the NiCo$_2$O$_4$@CNFs cathode with a higher loading mass, the discharge and charge processes of Li-O$_2$ batteries for the NiCo$_2$O$_4$@CNFs cathode with different loading mass at the same mass current density were performed shown in Fig. S11. The specific capacities of the NiCo$_2$O$_4$@CNFs cathode with loading mass of 0.134, 0.268, 0.536 mg cm^{-2} were 4179, 2231, 1992 mA h g^{-1}, respectively, and it can be clearly observed that the specific capacity decreased with the loading mass of the cathode increased. This result can be explained by two competing factors. First, at the specific current density, the larger the mass of the cathode, the higher the current density (I, in mA). It is known

that the smaller discharge capacities result from the higher current density. [S2, S3] So the cathode with higher loading mass is tested at higher current density, which results in the lower discharge capacity. Second, the higher mass loading or the thicker cathode, may show poor utilization efficiency of catalysts and poor mass transfer process leading to small discharge capacity. Therefore, we chose the low loading mass of the cathode to investigate the electrochemical performance of the $NiCo_2O_4$@CNFs.
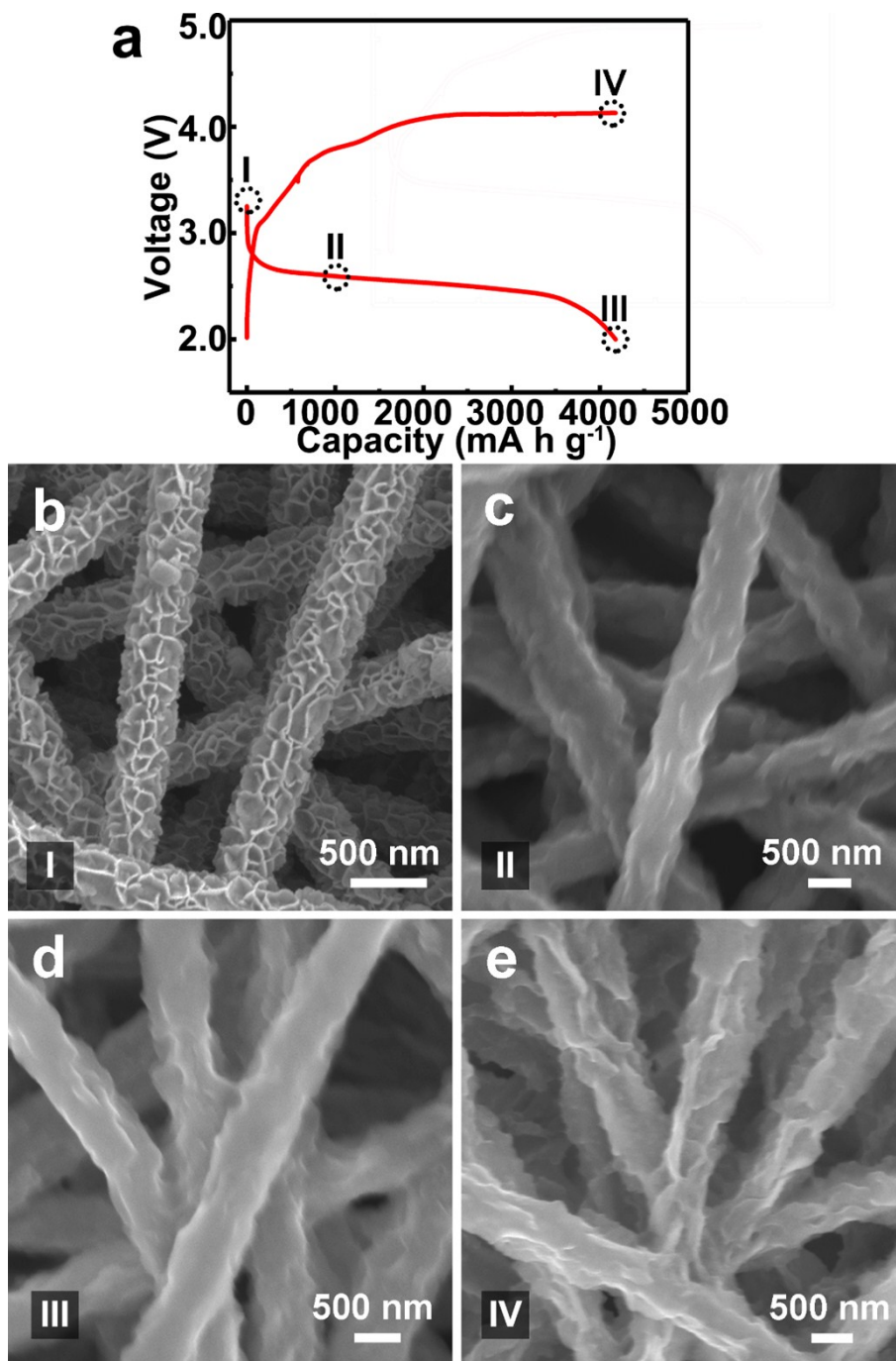
Fig. S8 a) Initial discharge/charge curves of Li-O$_2$ batteries for the NiCo$_2$O$_4$@CNFs cathode; b-e) The morphological changes of the NiCo$_2$O$_4$@CNFs cathode after 1st full discharge and 1st charge: b) before discharge, c) discharge to 1000 mA h g^{-1}, d) discharge to 2.0 V, e) after charge.
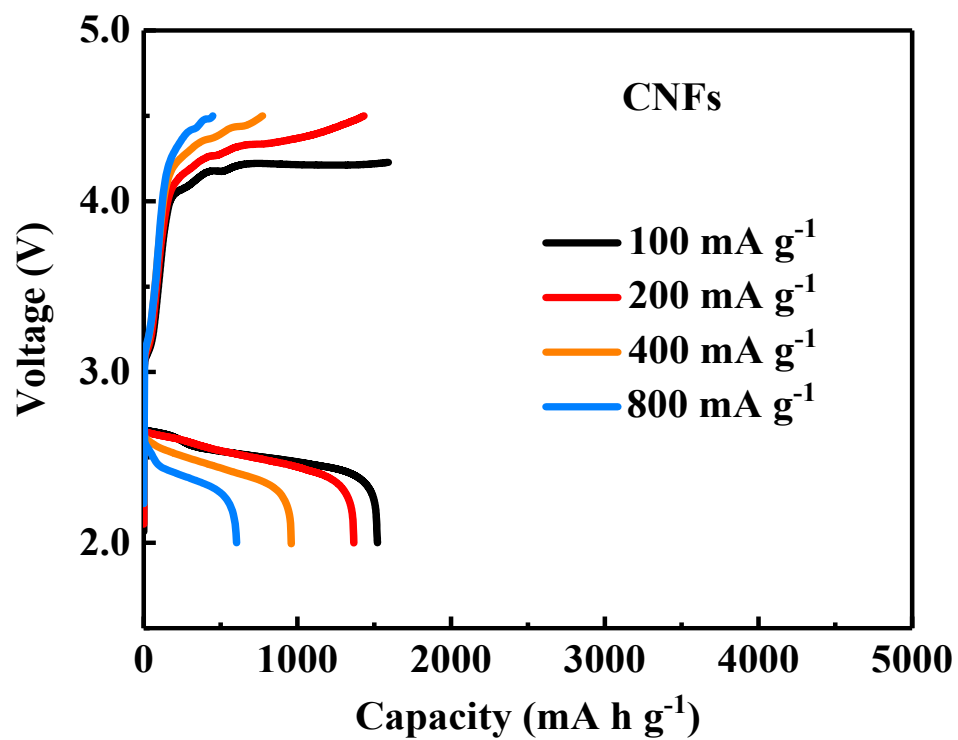
Fig. S9 Discharge/charge curves of Li-O$_2$ batteries with CNFs cathode at various current densities.
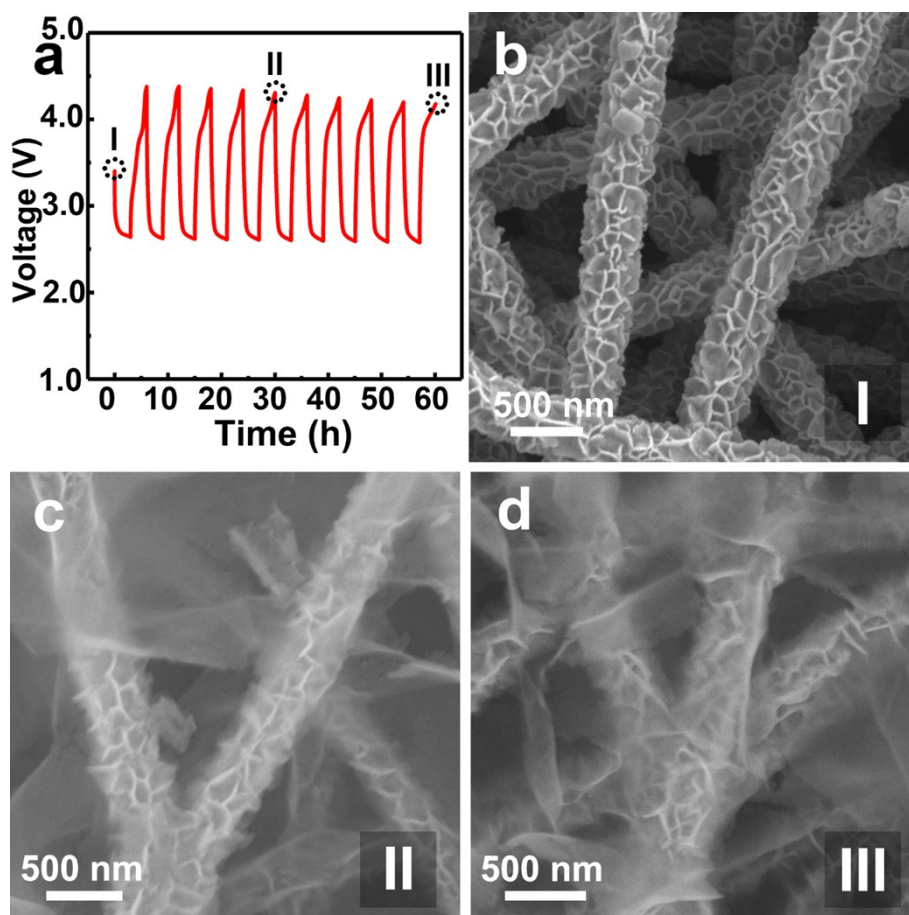
Fig. S10 a) The discharge/charge curves of Li-O$_2$ batteries for the NiCo$_2$O$_4$@CNFs cathode at a current density of 200 mA g^{-1} and a specific capacity limit of 1000 mA h g^{-1} during 10 cycles; b-d) The morphological changes of the NiCo$_2$O$_4$@CNFs cathode after the charge process: b) fresh cathode, c) after 5 cycles, d) after 10 cycles.

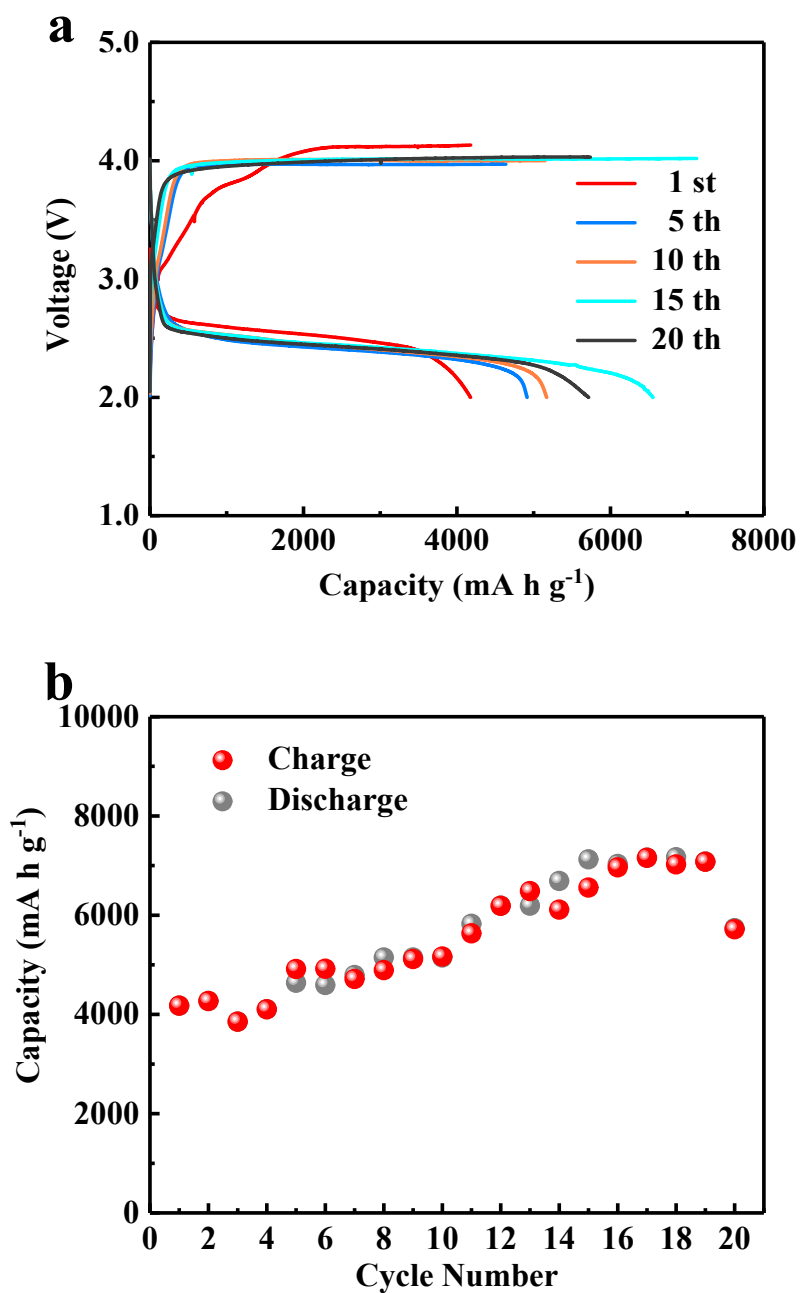**Fig. S11** a) Discharge-charge curves of Li-O$_2$ batteries with the NiCo$_2$O$_4$@CNFs cathode at a current density of 100 mA g^{-1} at full discharge/charge; b) Cycle performance of the NiCo$_2$O$_4$@CNFs cathode.

Table S1 Summary of Li-O$_2$ batteries performance with NiCo$_2$O$_4$-based cathodes.

Cathodes	Maximum Capacity	Loading Mass	Cycling performance	Limited Capacity	Binder	Ref.
NiCo$_2$O$_4$ @CNFs	**7168 mAh g^{-1}**	**40 % or 0.134 mg cm^{-2}**	**350 cycles at 200 mA g^{-1}**	**1000 mAh g^{-1}**	**binder free**	**This work**
NiCo$_2$O$_4$ nanoneedles @MnO$_2$	2372 mAh g^{-1}	3.0 % or 0.6 mg cm^{-2}	250 cycles at 100 mA g^{-1}	500 mAh g^{-1}	binder free	S4
Porous NiCo$_2$O$_4$@Ni	1535 mAh g^{-1}	4.3 % or 0.88 mg cm^{-2}	68 cycles at 0.05 mA cm^{-2}	800 mAh g^{-1}	binder free	S5
Ni Foam @ wave-like NiCo$_2$O$_4$	7004 mAh g^{-1}	2.3 % or 0.45 mg cm^{-2}	100 cycles at 100 mA g^{-1}	500 mAh g^{-1}	binder free	S6
PL-NiCo$_2$O$_4$ /Carbon Fabric	29279 mAh g^{-1}	1.8 % or 0.35 mg cm^{-2}	100 cycles at 0.1 mA cm^{-2}	1000 mAh g^{-1}	binder free	S7
NiCo$_2$O$_4$ Nanowires	4221 mAh g^{-1}	2.3% or ~0.45 mg cm^{-2}	200 cycles at 200 mA g^{-1}	1000 mAh g^{-1}	binder free	S8
NiCo$_2$O$_4$@N CF	5304 mAh g^{-1}	~11.2 %	92 cycles at 200 mA g^{-1}	500 mAh g^{-1}	binder free	S9
NiCo$_2$O$_4$ nanosheets	9026 mAh g^{-1}	40 %	50 cycles at 200 mA g^{-1}	1000 mAh g^{-1}	PTFE	S10
NiCo$_2$O$_4$@N-Graphene	6716 mAh g^{-1}	36 %	112 cycles at 200 mA g^{-1}	1000 mAh g^{-1}	PTFE	S11
NiCo$_2$O$_4$ nanorods	13250 mAh g^{-1}	50 %	15 cycles at 400 mA g^{-1}	1000 mAh g^{-1}	PTFE	S12
NiCo$_2$O$_4$ Nanowires	7600 mAh g^{-1}	15 %	50 cycles at 200 mA g^{-1}	1000 mAh g^{-1}	PVDF	S13
Urchin-like NiCo$_2$O$_4$	7309 mAh g^{-1}	30 %	33 cycles at 0.4 mA cm^{-2}	1000 mAh g^{-1}	PVDF	S14
NiCo$_2$O$_4$ nanotubes	5842 mAh g^{-1}	40%	100 cycles at 200 mA g^{-1}	1000 mAh g^{-1}	PVDF	S15
NiCo$_2$O$_4$@LSM nanorods	7992 mAh g^{-1}	15 %	80 cycles at 200 mA g^{-1}	1000 mAh g^{-1}	PVDF	S16
3D Foam-Like NiCo$_2$O$_4$	11376 mAh g^{-1}	50 %	80 cycles at 200 mA g^{-1}	1000 mAh g^{-1}	PVDF	S17

References

S1.   J. J. Xu, Z. L. Wang, D. Xu, F. Z. Meng and X. B. Zhang, *Energy Environ. Sci.*, 2014, **7**, 2213.

S2.   P. G. Bruce, S. A. Freunberger, L. J. Hardwick and J. M. Tarascon, *Nat. Mater.*, 2012, **11**, 19.

S3.   Y. Lin, B. Moitoso, C. Martinez-Martinez, E. D. Walsh, S. D. Lacey, J.-W. Kim, L. Dai, L. Hu and J. W. Connell, *Nano letters*, 2017, **17**, 3252.

S4.   A. Riaz, K. N. Jung, W. Chang, K. H. Shin and J. W. Lee, *ACS Appl. Mater. Interfaces*, 2014, **6**, 17815.

S5.   X. J. Lin, J. M. Su, L. Y. Li and A. S. Yu, *Electrochim. Acta*, 2015, **168**, 292.

S6.   C. Shen, Z. Y. Wen, F. Wang, K. Rui, Y. Lu and X. W. Wu, *J. Power Sources*, 2015, **294**, 593.

S7.   B. Liu, P. F. Yan, W. Xu, J. M. Zheng, Y. He, L. L. Luo, M. E. Bowden, C. M. Wang and J. G. Zhang, *Nano Lett.*, 2016, **16**, 4932.

S8.   H. R. Xue, S. C. Wu, J. Tang, H. Gong, P. He, J. P. He and H. S. Zhou, *ACS Appl. Mater. Interfaces*, 2016, **8**, 8427.

S9.   H. Xue, X. Mu, J. Tang, X. Fan, H. Gong, T. Wang, J. He and Y. Yamauchi, *J. Mater. Chem. A*, 2016, **4**, 9106.

S10.   B. Sun, X. Huang, S. Chen, Y. Zhao, J. Zhang, P. Munroe and G. Wang, *J. Mater. Chem. A*, 2014, **2**, 12053.

S11.   H. Gong, H. R. Xue, T. Wang, H. Guo, X. L. Fan, L. Song, W. Xia and J. P. He, *ACS Appl. Mater. Interfaces*, 2016, **8**, 18060.

S12.   B. Sun, J. Zhang, P. Munroe, H. J. Ahn and G. Wang, *Electrochem. Commun.*, 2013, **31**, 88.

S13.   F. Lu, X. Cao, Y. Wang, C. Jin, M. Shen and R. Yang, *RSC Adv.*, 2014, **4**, 40373.

S14.   H. S. Jadhav, R. S. Kalubarme, J. W. Roh, K. N. Jung, K. H. Shin, C. N. Park and C. J. Park, *J. Electrochem. Soc.*, 2014, **161**, A2188.

S15.   L. Y. Li, L. F. Shen, P. Nie, G. Pang, J. Wang, H. S. Li, S. Y. Dong and X. G. Zhang, *J. Mater. Chem. A*, 2015, **3**, 24309.

S16.   Y. Luo, F. L. Lu, C. Jin, Y. R. Wang, R. Z. Yang and C. H. Yang, *J. Power Sources*, 2016, **319**, 19.

S17.   L. L. Liu, J. Wang, Y. Y. Hou, J. Chen, H. K. Liu, J. Z. Wang and Y. P. Wu, *Small*, 2016, **12**, 602.